Biochemical and Biophysical Research Communications **268,** 155–163 (2000)
doi:10.1006/bbrc.1999.1934, available online at http://www.idealibrary.com on IDEAL®

Fluorescein Fluorescence Hyperpolarization as an Early Kinetic Measure of the Apoptotic Process

Naomi Zurgil, Zeev Schiffer, Yana Shafran, Menachem Kaufman, and Mordechai Deutsch[1]
The Jerome Schottenstein Cellscan Center for Early Detection of Cancer, Physics Department, Bar-Ilan University, Ramat-Gan 52900, Israel

Received November 22, 1999

The ability to identify apoptotic cells within a complex population is crucial in the research and diagnosis of normal physiology and disease states. The Cellscan mark *S* (CS-*S*) cytometer was used in this study to detect intracellular fluorescence intensity and polarization (FI and FP) in several well-established models of apoptosis: Following spontaneous apoptosis, as well as glucocorticoid or anti Fas-induced apoptosis, CS-*S* individual cell-based analysis revealed the appearance of a cell cluster characterized by low FI and high FP. Temporal analysis of annexine V binding and FP measurements following DXM treatment showed that hyperpolarization preceded phosphatidylserine appearance on the outer plasma membrane. The early increase in FP was found to be dose dependent and inversely related to cell diameter. Cell dehydration and alteration of plasma membrane transport properties, both occurring during early stages of apoptosis, may be involved in the phenomena of intracellular fluorescein hyper-polarization in apoptosis.

Key Words: **cellscan; apoptosis; fluorescence polarization; thymocytes.**

Apoptosis or regulated cell death is a physiological process of damaged or unwanted cell elimination, which ensures equilibrium between cell proliferation and cell death. Low level of apoptosis processes may result in malignancies, resistance to anti-cancer drugs and to autoimmune diseases. On the other hand, high level of apoptotic activity can result in immune deficiency or degenerative conditions. Hence, the recognition and quantitative measurements of apoptosis have become increasingly important for diagnosis and therapeutic monitoring.

Supported by the Horwitz Foundation Grant and by Medis-El Ltd., Yehud, Israel.

[1] To whom correspondence should be addressed. Fax: 972-3-5342019. E-mail: arnon-sh@actcom.co.il and cellscan@albert.ph.biu.ac.il.

Several assay systems have been developed to recognize and quantify apoptosis, including analysis of cell morphology, biochemical analysis, and flow cytometric methods.

Chromatin cleavage is the most characteristic biochemical feature of apoptosis. The appearance of the latter nucleosomal DNA fragments in agarose gel electrophoresis becomes the hallmark of apoptosis (1). *In situ* end labeling of fragmented DNA is used to measure DNA breaks in apoptotic cells in tissue section (2). This system has been adapted to flow cytometry (3).

Unfortunately, these biochemical techniques detect an averaged signal, which is obtained from cell suspension. Thus, a low reading might be the result of either a low expression across the entire population or a high expression originating only in a few cells, being masked by the negative majority of the population.

Flow cytometers and the Cellscan apparatus, on the other hand, measure individual cells, thus enabling the determination of apoptotic cell frequency. Moreover, heterogeneous cell populations with regard to cell types or cell cycle phase can be measured by selecting subpopulations or individual cells.

A variety of flow cytometric methods currently exist to analyze apoptotic cells (4–8). These assays can be grouped on the basis of the evaluated parameters used to define a cell as apoptotic:

a. Structural parameters, including cell size, shape, and granularity, chromatin structure, and DNA strand breaks. Most of these assays cannot be used to measure on intact living cells.

b. Functional apoptotic parameters measured in living cells include reduction in mitochondrial membrane potential, changes in intracellular pH and calcium ions, an increase in the level of superoxide anions and reactive oxygen intermediates, and augmentation in the activity of specific serine proteases.

Quantification of proteins involved in the apoptotic cascade like FAS or TNFR (9, 10) or intracellular proteins, including bcl-2, bax, c-mic p53 (11), and Apo 2.7

0006-291X/00 $35.00

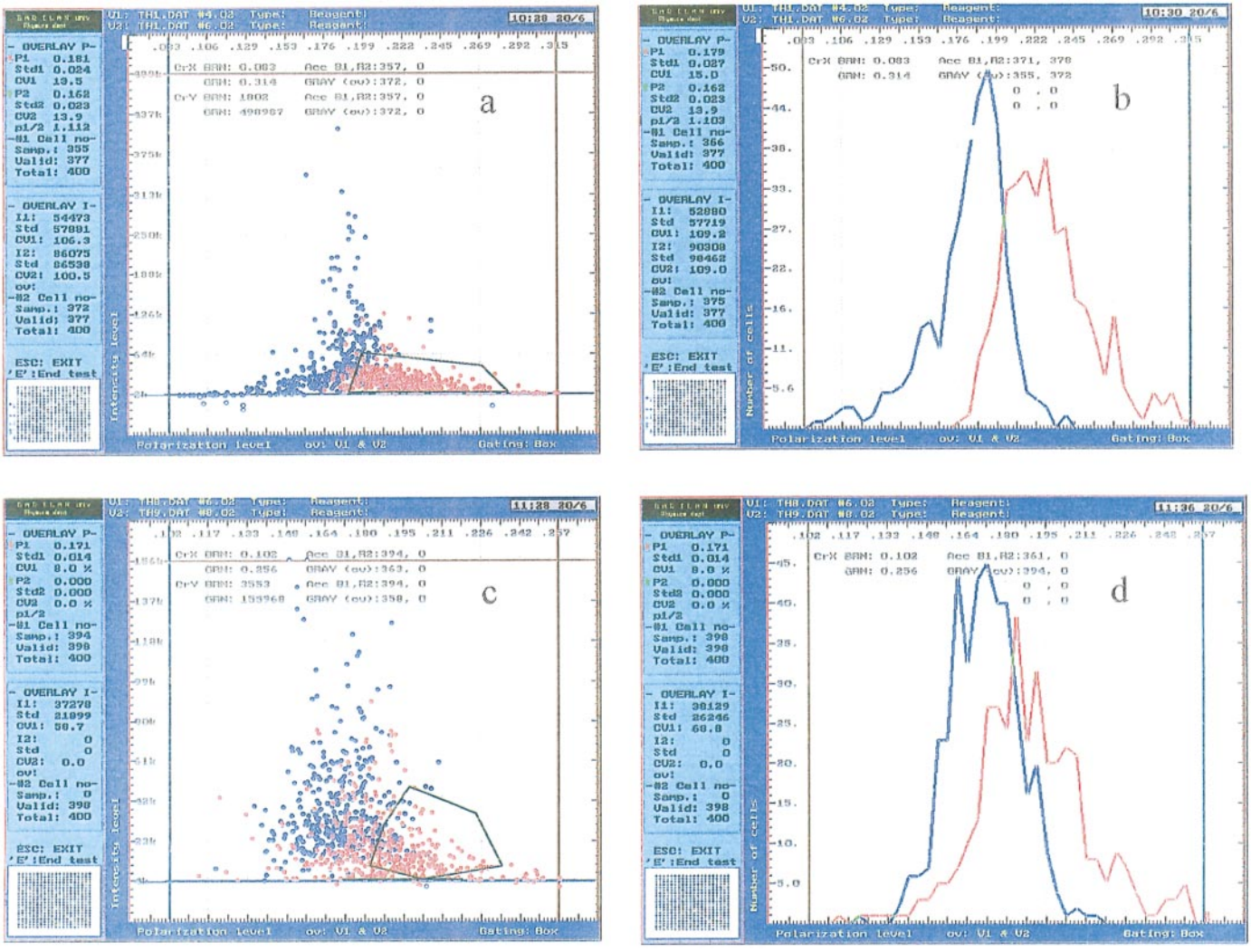

FIG. 1. Demonstration of apoptosis taking place in different cell types, by means of FI and FP measurements. (a) Scatter diagram of FI (vertical axis) vs FP (horizontal axis) of FDA labeled thymocyte individual values before (blue) and after (red) 24 h in culture. The HP cell cluster is defined by a polygon for further statistical analysis. (b) Distribution histogram of FP values of the same thymocyte populations shown in (a). (c) Scatter diagram of FI (vertical axis) vs FP (horizontal axis) of untreated (blue—control) or DXM-treated (1 μM for 4 h) (red) mouse thymocytes. (d) FP distribution histogram of the same cellpopulation shown in (c). (e) FI vs FP scatter diagram of Jurkat T cells following 3 h incubation with (red) and without (blue—control) DXM (0.1 μM). (f) Scatter diagram of FI (vertical axis) vs FP (horizontal axis) of untreated (blue) or anti-Fas-treated (1 μg/ml for 6 h) (red) mouse thymocytes. (g) FI vs FP scatter diagram of control Jurkat T cells (blue) and following 28 h of serum deprivation (red). (h) FP distribution histogram of the same cell population shown in (g).

(12), are also used to measure apoptosis. Annexine V is commonly used for staining phosphatidylserine, which is translocated from the inside to the outside the plasma membrane in the early steps of apoptosis (13).

The CS-*S* cytometer enables repeated measurement of individual intact living cells (14–16) and may thus serve as a suitable tool for monitoring the kinetics of the apoptotic process. In the present report the CS-*S* was used to detect intracellular fluorescein fluorescence intensity and polarization (FI and FP) in several well-established models of apoptosis. Both FI and FP provide quantitative measures of structural and biochemical changes which occur during early apoptosis.

The degree of FP is defined as $FP = (I_{\parallel} - I_{\perp})/(I_{\parallel} + I_{\perp})$, where $I_{\parallel}$ and $I_{\perp}$ are, respectively, the intensities of the parallel and perpendicular FP components relative to the excitation electric field vector. The more restricted the fluorescent probe mobility, the higher its FP, which is dictated by probe size, hosting media viscosity and binding.

MATERIALS AND METHODS

Materials. Propidium iodide (PI) and dexamethsone (DXM) were obtained from Sigma (St. Louis, MO). FDA was obtained from Riedle-de Haen AG (Seelze, Germany). Working dilutions (1.2 μM in PBS) were made from a 25 mM stock solution in acetic acid (Fruta-

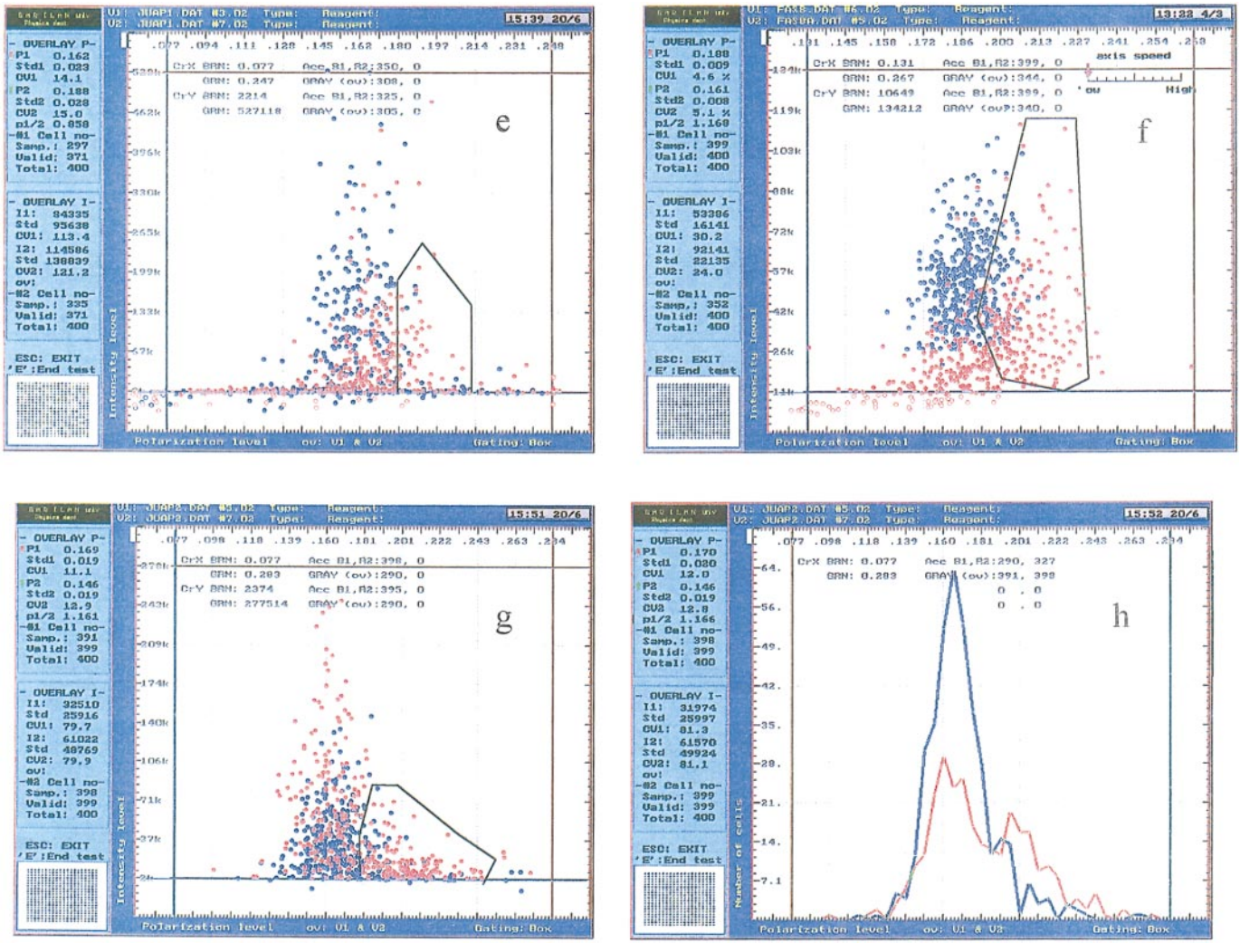

FIG. 1—*Continued*

rum, Israel), stored at room temperature for one week or less. Goat anti-mouse Fas antibodies were obtained from PharMingen (San Diego, CA). FITC-conjugated annexine V was obtained from Genzyme (Cambridge, MA).

Cell preparations. Mouse thymocytes were obtained from 2- to 3-week-old BALB/c male mice. Single thymocytes were prepared by mechanical disruption of freshly excised thymus. Suspensions were filtered, washed, and suspended in RPMI 1640 culture medium (Biological Industries, Israel) at a concentration of 1×10^6 cells/ml. Jurkat human T-lymphoblast cell line was grown as previously described (15, 17).

Apoptosis induction. Induction of spontaneous apoptosis was achieved by culturing thymocytes (5×10^6 cells/ml) in complete RPMI 1640 medium for 24 h. For DXM-induced apoptosis cells were incubated in complete RPMI 1640 medium in the presence of various concentrations of DXM for 0.5–24 h at 37°C. For serum-deprivation-induced apoptosis, Jurkat cells were washed twice with incomplete RPMI 1640 medium, then incubated in the same medium for 24 h. Apoptosis induction by anti-Fas was achieved by culturing mouse cells in the presence of anti-mouse Fas 1 μg/ml for 1–24 h at 37°C.

FDA staining. The cells were washed 3 times with incomplete RPMI 1640 medium without phenol red, containing 10 mM Hepes buffer solution. An aliquot of 50 μl of cell suspension (1–3 $\times$ 10^6 cells/ml) was added to 50 μl of staining solution of FDA in phosphate-buffered saline (PBS) and incubated at room temperature for 5 min. At the end of incubation, cells were settled in their well traps on the cell carrier as previously described (18), washed 3 times with fresh buffer to remove excess staining solution, and measured.

Plasma membrane integrity of FDA stained cells was checked by restaining the same cells with PI. At the end of FDA measurements, the cells were washed twice with fresh buffer, and a solution containing PI (2.5 μg/ml) was added on top of the pretested trapped cells for 5 min. Cells were then washed twice and another measurement was performed. Positive PI cells were excluded from the analysis.

Double staining with FITC-Annexine V and PI. One million cells were washed with PBS and resuspended in binding buffer (Genzyme, Cambridge, MA), FITC–annexine V was added at a final concentration of 1 μg/ml and PI was simultaneously added. After 10 min incubation in the dark at room temperature, cells were analyzed by flow cytometry (FACScan BD).

Viability test. Viability of cultured cells was determined by eosine exclusion test. Cells were incubated in the presence of eosine (0.1% in water) for 1 min.

TABLE 1

Morphological and Membranal Changes in Mouse Thymocytes Undergoing Spontaneous Apoptosis

Time (h)	% Dead cells (eosine)	% Annexine V positive	FSC (Au)	SSC (Au)	Nuclei area (μm^2)	FP	FI (Au)
0	1.2 ± 1.8	2.3 ± 1.7	524 ± 70	383 ± 81	10.9 ± 2.18	0.173 ± 0.018	47 ± 14.6
24	25.8 ± 4.3	14 ± 3.4	390 ± 55	457 ± 91	8.9 ± 2.55	0.197 ± 0.016	24 ± 9.5

Note. Fresh thymocytes were cultured in RPMI medium for 24 h in 37°C. Annexine V binding, FSC, and SSC were measured by FACS, nuclei area was measured by image analysis, and FI and FP of FDA labeled cells were measured by the CS-*S* cytometer. Au, arbitrary units.

Feulgen procedure. Cells were fixed on coverslips and stained with Shiff reagents as described (19).

Image analysis. Image analysis was performed using Scan Array 2 image analyser (Galai, Israel) (19). The quantitative parameters obtained by this system were the area of the nuclear profile and integrated optical density (IOD) related to the total DNA content.

CS-S apparatus. A detailed description of the CS-*S* apparatus has been given elsewhere (14–16).

Single cell morphological measurements. Minute and early morphological changes associated with apoptotic process were monitored by a unique single cell diffractocytometer described in detail elsewhere (20).

Statistical analysis. Data are expressed as means ± SD and were analyzed by two tailed paired Student's *t* test. Differences were taken to be significant at $P < 0.05$.

RESULTS

Apoptosis in thymocytes is a crucial event involved in the negative intrathymic selection of the T cell repertoire. It has been shown that thymocytes cultured for 24 h at 37°C in the absence of stimulation undergo apoptosis (21). Single thymocytes obtained from 2-week-old mice were cultured in medium, and then various apoptotic parameters including FI and FP were measured.

After 24 h in culture, about 25% of the cells were found dead, and 15% of the live thymocyte population were annexine V positive (Table 1). Significant alterations in FSC units, SSC, and the nuclei area were evident when measured by FACS and image analysis. Furthermore, changes appeared in the mean FI and FP values of the FDA-labeled thymocyte population; a significant decrease in FI concomitantly with an increase in FP.

The FI vs FP scatter diagram and the distribution pattern of FP values of individual cells within the thymocyte population after 24 h in culture compared with control at time 0 are shown in Figs. 1a and b, respectively.

A cell subgroup (defined by a polygon) characterized by low FI and high FP is apparent in the thymocytes undergoing spontaneous apoptosis. Restaining of the same cells with PI shows that this group of thymocytes excluded the dye PI, thus indicating membranal integrity (data not shown). Based on its comparison to the control scatter diagram pattern, this cluster of cells that exhibited high polarization values was defined as a responding one.

Similar high polarization (HP) cell clusters of cells were apparent in DXM (Figs. 1c and d) and anti Fas (Fig. 1f) treated thymus cells, as well in Jurkat T cells following either serum deprivation or DXM-induced apoptosis (Figs. 1e, g, and h, respectively).

Figure 2 shows the frequency of responding thymus cells as measured by the CS-*S*, following spontaneous, glucocorticoid, or anti-Fas-induced apoptosis. The percentage of cells in the high polarization cluster increased from 10% at the beginning of the test to 37% after 12 h in culture. Treatment of the thymocytes with either 1 μM DXM or anti-Fas antibodies resulted in a higher rate of responding cells than the spontaneously induced apoptotic cells, which was expressed by a similar HP appearing earlier in the course of cell death.

Figure 3 presents both annexine V binding and FP versus time in thymocytes and Jurkat T cells following DXM induced apoptosis. In both cell types, the increase in frequency of cells exhibiting hyperpolarization exceeds that of annexine V positive cells. After 5 h of DXM treatment, only about 10% of the thymocytes were positive to annexine V, whereas more than 50% showed HP. After 12 h, the majority of treated thymocytes showed HP, and only 23% demonstrated membrane asymmetry (Fig. 3a).

Cultured Jurkat T cells displayed different kinetic behavior (Fig. 3b). About 20% had already exhibited apoptotic parameters at time point 0. A sharp increase of up to 55% in the portion of cells possessing HP was evident during the first hour of DXM treatment, which thereafter decreased moderately (to 40%). Nevertheless, the frequency of annexine V binding cells was slower, reaching a maximum of about 26% after 6 h of exposure to DXM and decreased thereafter to about 10%. The frequency of viable cells in thymocytes and Jurkat populations exposed to DXM is shown in Fig. 3c. Indeed, the two cell types exhibited different death process kinetics. While most of the thymocytes show membrane integrity during the first 5 h of apoptosis induction, only 7 h later the percentage of live cells decreased dramatically reaching 90% 24 h from the beginning of the test. Cultured Jurkat T cells exhibited

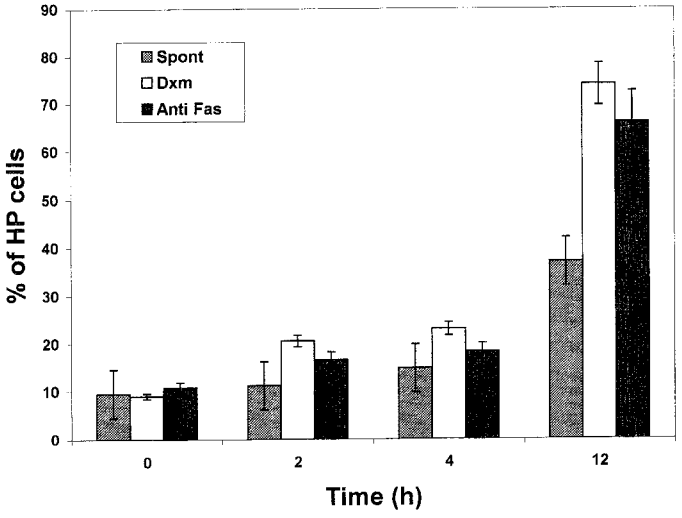

FIG. 2. Time dependence of HP cell cluster emergence. The percentage of HP thymus cells following spontaneous (gray bars) DXM (white bars) and anti-Fas (black bars)-induced apoptosis. The results are averages of three different experiments. The bars represent the corresponding SD of each set of experiment.

a rapid decrease in cell viability within the first 5 h of DXM exposure, but the number of dead cells leveled off at 50% after 12 h and increased thereafter.

Comparison between the kinetic assessment of DXM induced apoptosis (Figs. 3a and b) to the viability graph (Fig. 3c) indicates that the measure of FP might be more sensitive than annexine V in measuring apoptosis.

Figure 4 shows a dose–response curve of DXM-exposed thymus cells measured 30 min following induction of apoptosis. The treated cells showed no evidence of apoptosis as assessed either by sub G_0/G_1 subpopulation or by image analysis of the apoptotic nucleus. Furthermore, no changes were observed, neither in both cell size and granularity when measured by FSC and SSC in flow cytometry nor in the number of dead thymocytes as measured by the PI exclusion test. Still, as early as 30 min of DXM exposure, a significant change in HP cell count was evident, while no change at all was detected with annexine V, thus indicating that the FP increase of thymocytes preceded the appearance of phosphatidylserine on the outer plasma membrane. This early increase in FP of FDA labeled thymocytes was dose dependent, reaching a maximal value at 5 μM.

Hyperpolarization was also shown to occur earlier than annexine V binding when apoptosis was induced with anti-Fas antibodies (data not shown). An increase in FP value was evidenced after 3 h of anti-Fas treatment while annexine V positive cells were detected only after 6 h.

One of the early events in apoptosis is cell dehydration. This leads to cytoplasm condensation followed by a change in cell shape (6) and an increase in cytoplas-

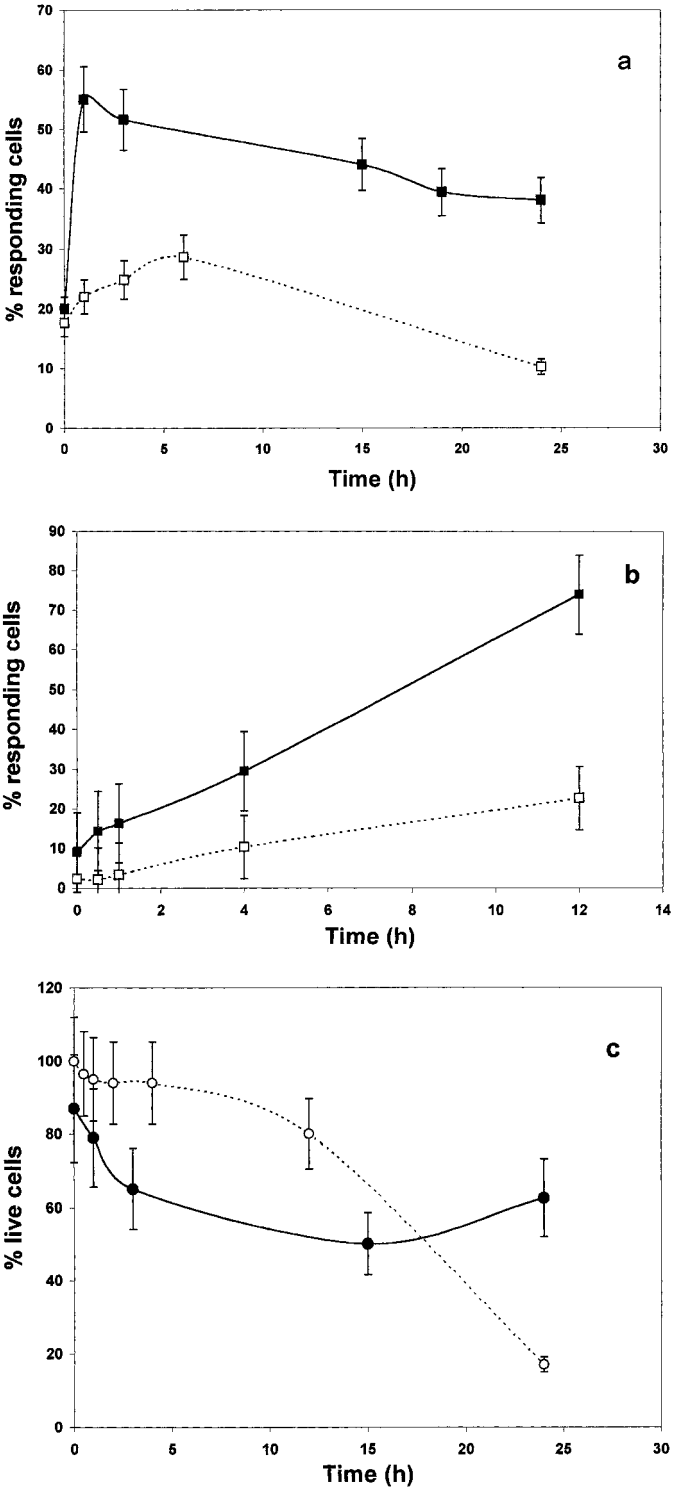

FIG. 3. Time-course analysis of apoptotic cells following DEX treatment. The percentage of annexine V (■) and high FP (□) positive cells in the Jurkat T cell line (a) and in fresh thymocytes (b) undergoing DEX-induced apoptosis. (c) Percentage of viable cells within these cell populations along the same period of DEX treatment. (○—thymocytes; ●—Jurkat T cells).

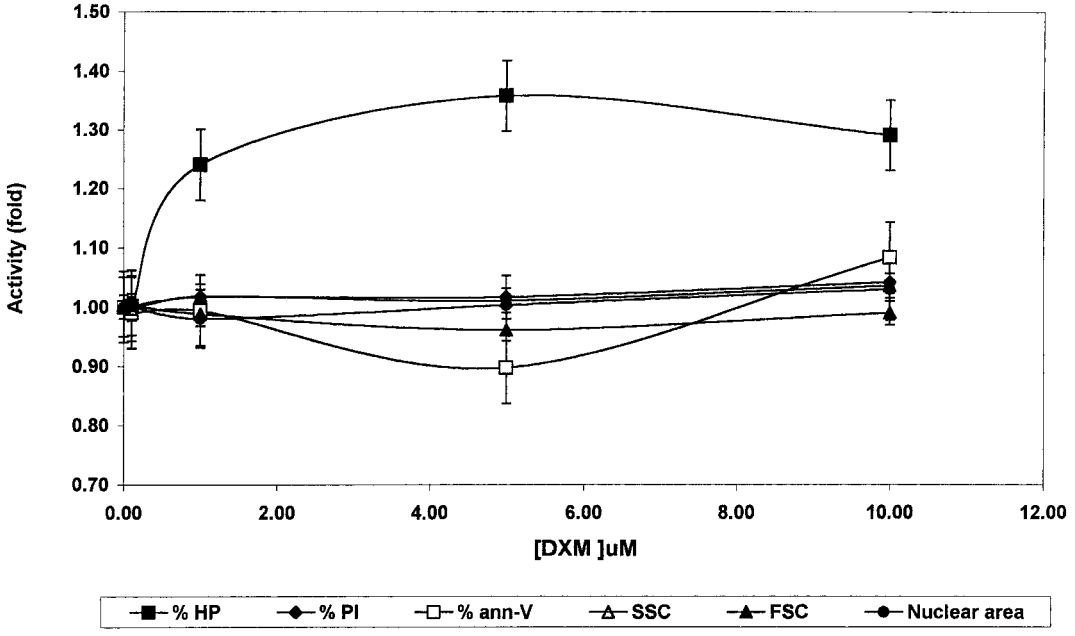

FIG. 4. DEX-induced apoptosis in thymocytes. DEX dose–response curves of mouse thymocytes. The response was measured 30 min following exposure to DEX and demonstrated by various parameters defined in the insert. SSC—side scatter, FSC—forward scatter. For further explanation see text.

mic viscosity. Morphological alterations taking place in thymocytes during early exposure to DXM could not be detected by FSC and SSC as measured by flow cytometer (see Fig. 4), but were detectable by the diffractocytometer, as discussed below.

Analysis of freshly isolated mouse thymus cells revealed a gaussian distribution histogram of cell diameter with a mean value of 7.5 ± 0.3 μm. Following DXM exposure, a subpopulation of smaller thymocytes having diameters between 6.2 and 7.1 μm was identified (data not shown).

The correlation between percentage of small size thymocytes and HP cells, measured in 5 different experiments of apoptosis induction by various DXM concentrations, is depicted in Fig. 5. The figure indicates that the change in FP was correlated with the changes observed in cell size. A linear correlation ($R^2 = 0.83$) was found between the percent of HP and of small cells.

Figure 6 illustrates the fact that cell shrinkage due to dehydration occurs concurrently with fluorescein hyperpolarization. Mouse thymocytes were suspended in 260, 280, or 300 mOsM PBS. Diffraction and FP measurements were performed. A reduction of mean diameter (from 7.35 ± 0.82 to 6.44 ± 0.42) and a simultaneous distribution shift in FP were evident (mean FP value of 0.159 ± 0.017 and of 0.185 ± 0.015 at 260 and 300 mosM, respectively).

DISCUSSION

The apoptotic response to various stimuli is an important part of cellular regulation, and the ability to identify apoptotic cells within a complex population is a prerequisite to a more detailed understanding of its role in normal physiology and in disease states.

Apoptosis is a dynamic process of variable duration. The time span during which the cell death process is identifiable varies depending on the method used, cell type, the cell cycle phase, or the nature of its inducing agent. Moreover, high variability exists within cell pop-

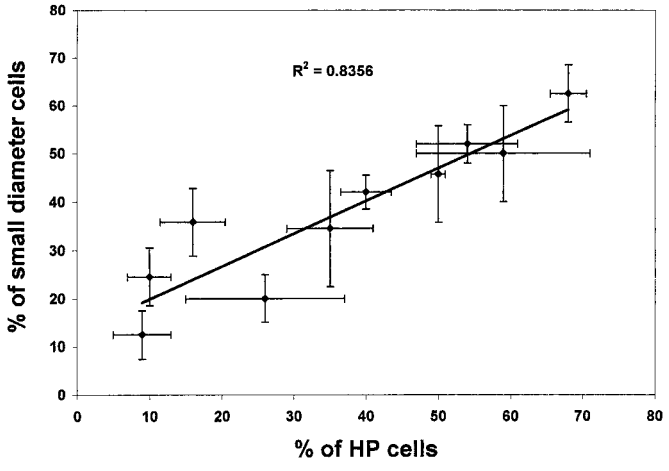

FIG. 5. Correlation between cell shrinkage and increase in FP following apoptotic induction. The mean percentage of small-diameter cell as a function of the mean percentage of HP cells within mouse thymocyte population undergoing DEX-induced apoptosis was obtained from 5 different experiments. In each experiment the measurements were performed in duplicate. The bars represent the corresponding SD of each set of experiment.

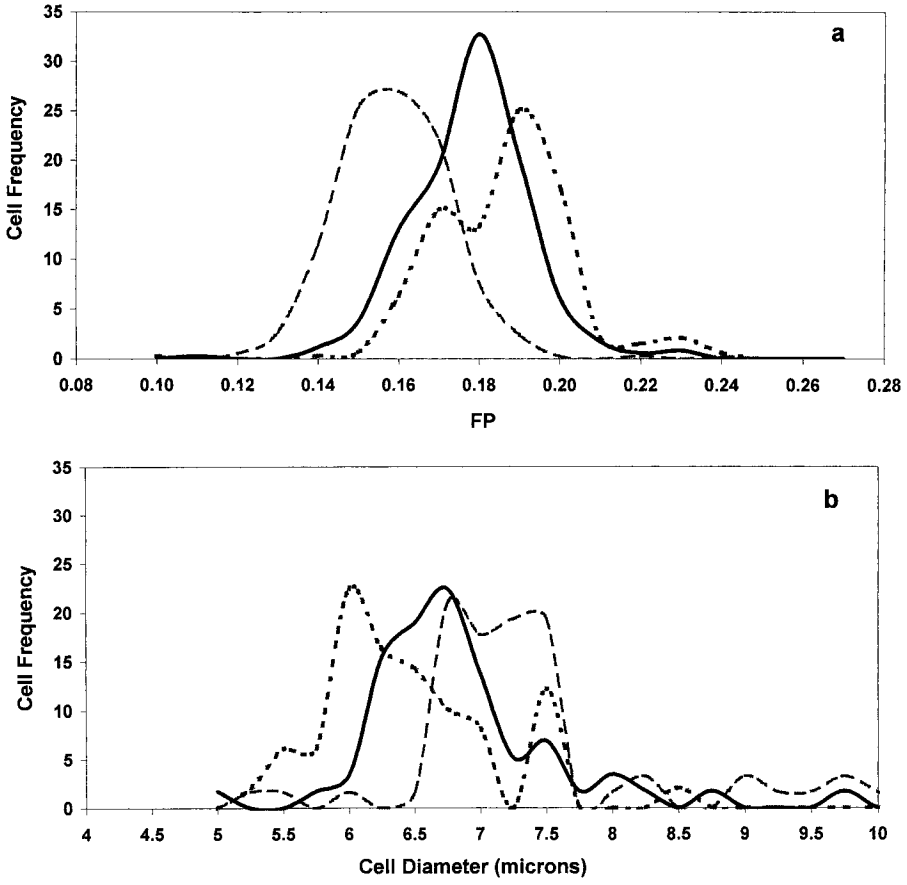

FIG. 6. Monitoring of cell dehydration induced by means of FP (a) and DLS (b). FP (a) and cell diameter (b) distribution histogram of fresh thymocyte population suspended in 260 (– – –), 280 (——), and 300 (· · ·) mosM PBS.

ulations with regard to the kinetics and the duration of the course of death (6, 22).

Flow-through and laser scanning cytometry (23) are being used to follow changes in the apoptotic cells and to quantify the number of these cells in culture, and recently also in clinical samples (22). Flow cytometry allows rapid analysis of large cell populations while laser scanning technology makes possible the correlation of fluorescence signals with visual microscopic morphology.

The CS-*S* cytometer allows repeated and high precision measurements to be made on the same individual intact living cells under physiological conditions over various periods of time (14–16). This feature is used to trace the kinetics of apoptotic events taking place in individual cells within a cell population as well as to classify subpopulations according to their measured parameters.

Since measurements and online cell manipulations (reagent addition, staining, changing buffers) are accomplished on the cell carrier (where cells are trapped and specifically localized) the cell loss as a result of detachment from the surface during late stages of apoptosis is negligible. Furthermore, an additional staining with a second probe (PI) at the end of measurements enabled the exclusion of dead cells.

The change in FI of FDA labeled cells is being used by others to monitor cell death (8, 24, 25). However, FI measurements of single cells depend on variables which may bias the results, such as intracellular fluorophore concentration, cell volume, cell trajectory, and position. Moreover, the CV (coefficient of variance) of FI values among cell population is high (about 65%). The FP level, being a measure of the fluorescent molecule rotational mobility level, is independent of FI, thus yielding smaller variation among cells ($\leq$10%).

FP measurements can provide considerable insight into the nature of macromolecular interactions, ligand binding, and conformational dynamics (16, 26, 27) as well as intracellular processing of protein (28).

Previous studies have shown that intracellular FP of FDA labeled T lymphocytes is cell cycle dependent, with significantly lower values for cycling than for noncycling populations (17, 29). Changes in FP of FDA-labeled lymphocytes have been shown to occur early in the course of lymphocyte activation triggered by mitogens (30–32) or antigens (33, 34).

This study provides evidence that the HP of intracellular fluorescein can be utilized as an early kinetic marker for apoptosis detection. The increase in the FP parameter was found to be ubiquitous, since it was demonstrated in several well-known models of cells undergoing apoptosis induced by various agents (i.e., serum-deprived and DXM-treated Jurkat T cells, cultured, DXM, and anti-Fas treated mouse thymocytes).

The intracellular HP coincided with morphological changes observed by light diffraction cytometer. A direct correlation ($R^2 = 0.83$) was found between the FP changes and the decrease in cell diameter. Moreover, manipulating the cells by changing the osmolarity caused structural alteration with a concomitant increase in FP values. In addition, a decrease in FI concurrently with FP changes of apoptotic cells was measured.

The biophysical aspects of fluorescein FP are thoroughly discussed elsewhere (35, 36). Several mechanisms may be involved in the phenomena of inracellular fluorescein HP in apoptosis: (1) cell dehydration increases the cytoplasmic viscosity, yielding a higher FP, which occurs during the early stages of apoptosis and is accompanied by cell shrinkage (6); (2) alteration in plasma membrane transport properties. The plasma membrane permeability of apoptotic cells is higher than that of normal cells (37). This results in a higher rate of DNA binding dyes uptake (37–40), and may affect esterase substrates influx as well as their hydrolyzed products efflux (37, 41). In this respect, efflux enhancement may shift the equilibrium ratio between "free" and "rotationally restricted" intracellular fluorescein towards the "rotationally restricted" state, thus yielding a higher FP.

Hyperpolarization due to intracellular viscosity induced solute/solvent interaction was ruled out (36). Such interactions may enhance the non radiating energy transitions which shorten the actual fluorescence decay time, causing higher FP.

Furthermore, the degree of acidification associated with apoptosis is sufficient to influence both absorption and emission spectra of the intracellular fluorescein but not its FP (36).

Detection of early cellular responses occurring during the apoptotic cascade is of great importance because of the ability to monitor the death process at an early stage where it may still be reversible and can be modulated. Moreover, since the early apoptotic phase is already associated with surface changes that allow recognition by macrophages, it is very likely that the apoptotic cells found *in vivo* before phagocytosis occurs are mostly those in the early phase.

This cell surface exposure of PS during apoptosis serves for recognition and removal of the dying cell by phagocytes. It has been shown that murine thymocytes incubated in the presence of DXM first start to expose PS at their cell surface while the plasma membrane still remains intact (42–44). In neuronal cells, however, externalization of PS is a late apoptotic event which coincided with the loss of surface adhesion and the phagocytosis by microglia (45). Moreover, several models of apoptosis showed no change in annexine V binding (8).

In the current study externalization of PS by mouse thymocytes was found to be an early signal of apoptosis preceding the plasma membrane and nuclear changes. Moreover, HP in FDA labeled cells was shown to appear earlier than the PS exposure and a more sensitive measure for early apoptosis. Hyperpolarization in Jurkat T cells exposed to DXM was also shown to detect apoptosis at an early kinetic time point, prior to annexine V binding.

Time dependency analysis of FP in thymocytes and Jurkat lymphocytes revealed that the two cell types exhibited different kinetics of DXM-induced apoptosis. Such a difference may be attributed to the variation in cell cycle regulation of the death process. It has been shown that in murine thymocytes DXM kills a broad spectrum of the CD4/8 immunophenotypes with no selectivity for cell cycle stage (7), whereas in human T cells, cell cycle control of apoptosis was found for both leukemic (46) and mature T lymphocytes (47, 48).

The current study implies that analysis of FP by the CS-*S* cytometer can provide an additional quantitative and sensitive tool for monitoring early biophysical changes taking place in cells undergoing apoptosis and may be used in the study of the mechanism involved in the apoptotic process.

REFERENCES

1. Cohen, J. J. (1993) *Immunol. Today* **6,** 126–130.
2. Gavrieli, Y., Sherman, Y., and Ben-Sasson, S. A. (1992) *J. Cell. Biol.* **119,** 493–501.
3. Groczyca, W., Gong, J., and Darzynkiewicz, Z. (1993) *Cancer Res.* **53,** 1945–1951.
4. Darzynkiewicz, Z., Bruno, S., Del Bino, G., Gorczyca, W., Hotz, M. A., Lassota, P., and Traganos, F. (1992) *Cytometry* **13,** 795–808.
5. Dive, C., Gregory, C. D., Phipps, D. J., Evans, D. L., Milner, A. E., and Wyllie, A. H. (1992) *Biochim. Biophys. Acta* **1133,** 275–285.
6. Darzynkiewicz, Z., Xun Li, G. J., Gorczyca, W., Murakami, T., and Traganos, F. (1977) *Cytometry* **27,** 1–20.
7. Chiu, L., Cherwinski, H., Ransom, J., and Dunne, J. F. (1996) *J. Immunol. Methods* **189,** 157–171.
8. Frey, T. (1997) *Cytometry* **28,** 253–263.
9. DiGiuseppe, J. A., LeBeau, P., Augenbraun, J., and Borowitz, M. J. (1996) *Am. J. Clin. Pathol.* **106,** 345–351.
10. Molica, S., Mannella, A., Dattilo, A., Levato, D., Iuliano, F., Peta, A., Consarino, C., and Magro, S. (1996) *Haematologica* **81,** 302–309.
11. Steck, K., McDonnell, T., Sneige, N., and el-Naggar, A. (1996) *Cytometry* **24,** 116–122.
12. Koester, S. K., Roth, P., Mikulka, W. R., Schlossman, S. F., Zhang, C., and Bolton, W. E. (1997) *Cytometry* **29,** 306–312.

13. Vermes, I., Haanen, C., Steffens-Nakken, H., and Reutelingsperger, C. (1995) *J. Immunol. Methods* **184,** 39–51.
14. Sunray, M., Kaufman, M., Zurgil, N., and Deutsch, M. (1999) *Biochem. Biophys. Res. Commun.* **261,** 712–719.
15. Deutsch, M., Kaufman, M., Shapiro, H., and Zurgil, N. (1999) *Cytometry* **39,** in press.
16. Zurgil, N., Kaufman, M., Solodiev, In., and Deutsch, M. (1999) *J. Immunol. Methods* **8411,** in press.
17. Zurgil, N., Deutsch, M., Tirosh, R., and Brodie, C. (1996) *Cell Struct Funct* **21,** 271–276.
18. Deutsch, M., and Weinreb, A. (1994) *Cytometry* **16,** 214–226.
19. Shneyvays, V., Hawrath, K., Jacobson, A., and Shinberg, A. (1998) *Exp. Cell Res.* **243,** 383–397.
20. Schiffer, Z., Ashkenazy, Y., Tirosh, R., and Deutsch, M. (1999) *Appl. Opt.* **38,** 3626–3635.
21. Petit, P. X., Lecoeur, H., Zorn, E., Dauguet, C., Mignotte, B., and Gougeon, M. L. (1995) *J. Cell Biol.* **130,** 157–167.
22. Bender, E., Li, X., Gorczca, W., Melamed, M. R., and Darzynkiewicz, Z. (1999) *Cytometry* **35,** 181–195.
23. Dowsett, M., Detre, S., Ormerod, M. G., Ellis, P. A., Mainwaring, P. N., Titley, J. C., and Smith, I. E. (1998) *Cytometry* **32,** 291–300.
24. Lizard, G., Furnel, S., Genestier, L., Dhedim, N., Chaput, C., Flacher, M., Mutin, M., Panaye, G., and Revillard, J. P. (1995) *Cytometry* **21,** 275–283.
25. Satoh, T., Sakai, N., Kubo, T., Enokido, Y., Uchiyama, Y., and Hatanaka, H. (1995) *Neurosci. Lett.* **201,** 119–122.
26. Carrero, J., Mallender, W. D., and Voss, E. W., Jr. (1996) *J. Biol. Chem.* **271,** 11247–11252.
27. Thevenin, B. J., Periasamy, N., Shohet, S. B., and Verkman, A. S. (1999) *Proc. Natl. Acad. Sci. USA* **91,** 1741–1745.
28. Weaver, D. J., Jr., Durack, G., and Voss, E. V., Jr. *Cytometry* **28,** 25–35.
29. Cercek, L., and Cercek, B. (1978) *Biophys. J.* **23,** 395–405.
30. Eisenthal, A., Marder, O., Lifschitz-Mercer, B., Skornick, Y., Fixler, D., Avtalyon, R., Tirosh, R., and Deutsch, M. (1997) *Pathobiology* **65,** 69–74.
31. Kaplan, M. R., Trubniykov, E., and Berke, G. (1997) *J. Immunol. Methods* **201,** 15–24.
32. Deutsch, M., Zurgil, N., Kaufman, M., and Berke, G. (1999) *in* T Cell Protocols: Development and Activation (K. Kearse, Ed.), Humana Press, Totowa, NJ (in press).
33. Zurgil, N., Gerbat, S., Langevitzh, P., Tishler, M., Ehrenfeld, M., and Shoenfeld, Y. (1997) *Isr. J. Med. Sci.* **33,** 273–279.
34. Zurgil, N., Levy, Y., Deutsch, M., Gilburd, B., George, J., Haratz, D., Kaufman, M., and Shoenfeld, Y. (1999) *Clin. Cardiol.* **22,** 526–532.
35. Gellman Zhornitsky, E., Deutsch, M., Tirosh, R., Yitshak, Y., Weinreb, A., and Shapiro, H. (1997) *J. Biomed. Opt.* **2,** 186–194.
36. Fixler, D., Deutsch, M., and Eisenthal, A. (1998) *J. Biomed. Opt.* **3,** 312–325.
37. Ormerod, M. G., Sun, X.-M., Snowden, R. T., Davies, R., Fearnhead, H., and Cohen, G. M. (1993) *Cytometry* **14,** 595–602.
38. Frey, T. (1995) *Cytometry* **21,** 265–274.
39. Schmid, I., Uitenbogaart, C. H., and Giorgi, J. V. (1994) *Cytometry* **15,** 12–20.
40. Idziorek, T., Estaquier, J., De Bels, F., and Ameisen, J.-C. (1995) *J. Immunol. Methods* **185,** 249–258.
41. D'Mello, S. R., Anelli, R., and Calissano, P. (1994) *Exp. Cell Res.* **211,** 332–338.
42. Stuart, M. C., Damoiseaux, J. G., Fredrick, P. M., Arends, J. W., and Reutelingsperger, C. P. (1998) *Eur. J. Cell Biol.* **76,** 77–83.
43. van Engeland, M., Nieland, L. J., Ramaekers, F. C., Scutte, B., and Reutelingsperger, C. P. (1998) *Cytometry* **31,** 1–9.
44. Donner, K. J., Becker, K. M., Hissong, B. D., and Ansar, A. (1999) *Cytometry* **35,** 80–90.
45. Adayev, T., Estephan, R., Meserole, S., Mazza, B., Yurkov, E. J., and Banerjee, P. (1998) *J. Neurochem.* **71,** 18854–18864.
46. Novelli, F., Allione, A., Wells, V., Forni, G., and Mallocci, L. (1999) *J. Cell Physiol.* **178,** 102–108.
47. Tuosto, L., Cundari, E., Montani, M. S., and Piccolella, E. (1994) *Eur. J. Immunol.* **24,** 1061–1065.
48. Algeciras-Schimnich, A., Griffith, T. S., Lynch, D. H., and Paya, C. V. (1999) *J. Immunol.* **162,** 5205–5211.